Fig. S1. Further characterization of PSD95 and mutated PSD95 FRET sensors.

A) Schematic of PSD95 (Ch-PSD95-V) and mutated PSD95 (C3,5S-Ch-PSD95-V) FRET sensor constructs as in Figure 1A.

(B) Ch-PSD95-V is palmitoylated. Ch-PSD95-V was expressed in HEK293 cells and assayed for palmitoylation by the acyl-biotin exchange (ABE) assay. *Top*: ABE assay comparing sham-transected HEK293 cells (sham) and cells transfected with Ch-PSD95-V. Specific labeling was only observed with the hydroxylamine (HAM) treatment step, a step required in the ABE method to assay for palmitoylation. *Bottom*: Total cellular expression of Ch-PSD95-V was assayed by Western blots.

(C) Distribution of Ch-PSD95-V and C3,5S-Ch-PSD95-V in dendrites. *Left panels*, cultured hippocampal neurons were transfected with Ch-PSD95-V (*top*) or C3,5S-Ch-PSD95-V (*bottom*). Displayed are images of mCherry fluorescent signal in dendrites for each construct. Ch-PSD95-V concentrated in spines, consistent with WT PSD95 distribution. C3,5S-Ch-PSD95-V had a more diffuse distribution consistent with disrupted targeting and accumulation at spines. Scale bar represents 5 µm. *Right panels*, (insets of dashed boxes in left panels) distribution of Ch-PSD95-V and C3,5S-Ch-PSD95-V at synapses. Neurons were fixed and immunolabeled with anti-Bassoon antibody to identify presynaptic sites. Ch-PSD95-V, but not C3,5S-Ch-PSD95-V, co-localized with anti-Bassoon staining.

Fig. S2. Ch-PSD95-V FRET in HEK293 cells.

(A) Representative images of the photobleaching method performed on Ch-PSD95-V in HEK293 cells to obtain Ch-PSD95-V intramolecular FRET efficiency (*top 3 panels*). Venus and mCherry fluorescence images were acquired before and after 6 acceptor photobleaching steps. Bottom row displays Venus (donor) pseudo-color intensity. No rise in donor intensity is observed when Ch-PSD95 is co-expressed with PSD95-V (*bottom 3 panels*).

(B) Ch-PSD95-V FRET efficiency determined from the linear relationship between increases in donor (mCherry) fluorescence with decreases in acceptor (Venus) with photobleaching. The photobleaching steps for ChPSD95-V in (A) are plotted as the percent decrease in acceptor intensity versus the percent increase in donor intensity (black circles). A corresponding rise in donor intensity is not observed when Ch-PSD95 is co-expressed with PSD95-V (open circles).

(C) FRET efficiency values, E_T, were calculated from the data above using the equation: $E_T = (1 - I_{da}/I_d)$, where I_{da} and I_d are the fluorescence intensities of the donor in the presence and absence of acceptor, respectively. FRET efficiency for Ch-PSD95-V is 17.7% ± 0.4% (mean ± SEM; n= 27 cells, *p<0.00001) compared to 0.9% ± 0.7% (mean ± SEM; n= 19 cells) in cells co-expressing Ch-PSD95 and PSD95-V.

Fig S3. Palmitoylation conditions for Ch-PSD95-V FRET measured in HEK293 cells. Representative images of cells used for the Ch-PSD95-V FRET analysis in Figure 1B to test for changes in conformation and palmitoylation. Images are displayed from HEK293 cells expressing Ch-PSD95-V or C3,5S-Ch-PSD95-V (*top rows*), with Myc-DHHC15 (*third and fourth rows*), Myc-DHHC2 (*fifth row*), palmostatin B treatment (*sixth row*), or palmostatin B treatment and Myc-DHHC2 expression (*bottom row*). Shown are initial and final (Pre and Post) Venus and mCherry fluorescence signals acquired over the course of acceptor photobleaching. Epitope-tagged DHHC proteins were detected with anti-Myc antibodies (blue). Scale bar represents 10 μm.

Fig S4. Loss of PSD95 palmitoylation alters co-precipiatation and co-localization with NMDAR subunits.

(A) 2-Bromopalmitate (2-BP) treatment prevents co-localization between NMDAR subunits and PSD95. HEK293 cells expressing HA-NMDAR and PSD95-GFP were untreated (*left*) or treated with 2-BP (*right*). PSD95 was visualized via its GFP tag, and immunostaining with anti-HA antibody was used to visualize NMDARs.

(B) PSD95 C3,5S mutation reduces PSD95 interactions with GluN2B. To assay PSD95-NMDAR interactions in a cell system, PSD95-GFP, wild-type [WT] or C3,5S mutant, were co-expressed (Co-Exp) with the NMDAR subunit, GluN2B, in COS7 cells. To assay *in vitro* interactions, PSD95-GFP and GluN2B were expressed separately in two sets of HEK293 cells and their lysates mixed post-solubilzation (P.Sol). PSD95 constructs in cell lysates were immunoprecipitated with anti-GFP antibody and analyzed on Western blots with anti-GluN2B and anti-PSD95 antibodies. Displayed are representative Western blots.

(C) PSD95 C3,5S mutation inhibits PSD95 interactions with NMDARs. PSD95-GFP (WT or C3,5S mutant) and NMDAR subunits, GluN2B and HA-GluN1, were co-expressed in HEK293 cells. Lysates were prepared and PSD95 constructs immunoprecipitated with anti-GFP antibody and probed with anti-GluN2B, anti-HA, and anti-PSD95 antibodies. Displayed are representative Western blots.

(D, E) The palmitoylation inhibitor, 2-BP, blocks PSD95 interactions with GluN2B subunits. PSD95-GFP was expressed in HEK293 cells, treated with 2-BP (100 μM), lysates prepared and mixed with lysates from cells expressing GluN2B (D). Alternatively, PSD95-GFP and GluN2B were co-expressed and cells were treated with 2-BP (E). Lysates were processed as described in (B). Displayed are representative Western blots.

(F) 2-bromopalmitate inhibits PSD95 and NMDAR interactions. PSD95-GFP and NMDARs were co-expressed in HEK293 cells, treated with 2-BP (100 μM), and lystates were prepared as described in (B). Displayed are representative Western blots.

(G) Quantification of band intensity changes for co-precipitation of PSD95 or C3,5S- PSD95 with NMDAR subunits. Quantification of effects of C3,5S mutation or 2-BP treatment (100 μM) on interaction between PSD95 and GluN2B/NMDARs. C3,5S mutation caused GluN2B and PSD95 co-IP to decrease to 15.2% ± 1.4% when the interaction occurs in vitro and 15.8% ± 1.5% when the interaction occurs in cells. 2-BP treatment decreased the co-IP to 15.0% ± 0.4% (*in vitro*) and 34.3% ± 11.4% (in cells). For NMDAR-PSD95 interactions, C3,5S mutation decreased co-IP to 15.8% 0.3% and 2-BP treatment decreased the co-IP to 34.2% ± 5.8%. Data are expressed as mean ± SEM for 4 experiments per condition.

Fig S5. Further analysis of the role of PSD95 palmitoylation in regulating interactions with AMPARs.

Additional quantification for the experiments displayed in Fig. 2F, which demonstrated that loss of PSD95 palmitoylation sites disrupted interactions between PSD95 and AMPARs containing Stargazin. Band intensities from 4 separate Western blots were used in the analysis and are plotted as the percent of wild type (WT) PSD95, with Ch-PSD95-V set at 100% when immunoprecipitated with Stargazin alone. The mean value for C3,5S-Ch-PSD95-V band intensities was 22.8 ± 4.5% (SEM) with Stargazin alone, and the mean values for Ch-PSD95-V and C3,5S-Ch-PSD95-V when immunoprecipitated with Stargazin and GluA1 were 67.3% ±10.3% and 1.5% ± 0.5%,respectively, *$p < 0.001$.

SUPPLEMENTAL EXPERIMENTAL PROCEDURES

Culture of HEK293 cells and primary hippocampal neurons. HEK-293 cells were maintained in DMEM supplemented with 10% calf serum (Hyclone). Cells were transiently transfected with cDNA using a calcium phosphate protocol (1). Cells transfected with HA-GluR1 or HA-NMDAR were maintained in media containing 1 mM kynurenic acid (Sigma) or 100 M D(-)-2-amino-5-phosphonovaleric acid (Sigma) and 10 M MK-801 (RBI), respectively, to prevent excitotoxicity. Hippocampal cultures were prepared using Neurobasal Media (NBM), 2% (v/v) B27, and 2 mM L-glutamine. Briefly, hippocampi from embryonic (E18–19) Sprague-Dawley rats were dissected, dissociated in 0.05% trypsin (vol/vol, Invitrogen), and cells were plated at a density of □4 × 10^5 cells/mL on polyethylenimine-coated 12-mm coverslips. Coverslips were maintained in Neurobasal media containing B27 and GlutaMAX (all from Invitrogen). Neuronal cultures were transfected at 12–14 DIV with the Lipofectamine 2000 transfection reagent

(Invitrogen), according to manufacturer's recommendations, with the exception that 1–2.5 g of each cDNA in 62.5 µl of Neurobasal media and 2.5 µl of Lipofectamine 2000 in 62.5 µl of Neurobasal media were mixed and added to coverslips in 12-well plates.

Antibodies and Reagents. The following antibodies were used: Anti-Bassoon antibody (Synaptic Systems), anti-PSD95 antibodies (Stressgen or Neuromab), anti-NR2B antibody (BD Biosciences), anti-GluA1 antibody (Calbiochem), anti-GluA2 antibody (EMD Millipore), anti-HA (rabbit polyclonal) antibody (Bethyl Laboratories), anti-Myc 9E10 antibody (Santa Cruz Biotechnology), anti-GFP antibody (Sigma-Aldrich). Alexa Fluor anti-rat 488/568, Alexa Fluor anti-rabbit 647, Alexa Fluor anti-rabbit 750, Alexa Fluor anti-Mouse 647, and Alexa Fluor anti-Mouse 750 were purchased from Molecular Probes (Eugene, OR).

Plasmids and Transfections. Rat GluN1 and GluN2B were obtained from J. Boulter (University of California, Los Angeles). GluN1 and GluN2B subunits were tagged at the NH_2 terminus with the FLAG (DYKDDDDK) and HA (YPYDVPDYA) epitopes, respectively, using the extension overlap PCR method (2) and subcloned into a pCB6 mammalian expression vector. Construction of GFP- SAP97□ (splice variant I1b, I3 and I5) has been previously described (3, 4). To generate Ch-SAP97-V, *EcoRI* restriction enzyme sites were placed on the N- and C-termini of mCherry and *KpnI* sites were placed on the N- and C-termini of Venus using PCR. Using *EcoR1* and *KpnI*, mCherry and/or Venus were subcloned into SAP97□ in pEGFP-N1 and screened for correct directional insertion. To generate Ch-PSD95-V, Cherry-PSD95, and PSD95-Venus, *EcoR1* sites were place on either end of mVenus (in pCS2) and subcloned in frame by restriction digest into *EcoR1* site in PSD95-GFP (in pGW1) to generate PSD95-Venus. A *KpnI* site was introduced within the N-terminus of PSD95α by a C to G point mutation to base pair 39 using Quikchange (Invitrogen). PCR was used to attach KpnI sites to the ends of mCherry and mCherry was subcloned into PSD95-V or PSD95α to generate Ch-PSD95 or Ch-PSD95-V respectively. C3,5S mutations were introduced by G to C point mutations in residues 3 and 5 using Quikchange. cDNA encoding PF11-GFP (PSD95 intrabody) was obtained from M. Fukata (National Institute for Physiological Sciences, Japan) and F. Perez (Institut Curie Centre de Reserche, France).

Immunostaining and Image Analysis. HEK-293 cells and neuronal cultures (24 h post-transfection) were washed twice in phosphate-buffered saline (PBS) at 22–25 °C, fixed in 4% paraformaldehyde/sucrose (vol/vol, RT, 15 min) and washed three times in PBS (5–10 min). For permeabilization, cells were incubated in 0.1% Triton-X in PBS (10 min), incubated in blocking solution (2% glycine (wt/vol), 2% BSA (wt/vol), 0.2% gelatin (wt/vol) and 50 mM NH_4Cl in 1 PBS; 10 min) and then incubated with the indicated primary antibody diluted in blocking solution (1 h).

For surface labeling, the permeabilization step was omitted and primary antibody incubation was overnight at 4°C. Following primary antibody incubation, cells were washed three times in blocking solution (5–10 min) and overlaid with an appropriate secondary antibody diluted in blocking solution (1 h). Cells were then washed three times in PBS (5–10 min) and the slips mounted in 80% glycerol or Prolong Gold (Invitrogen). Fluorescence images were acquired using a Leica SP5 Tandem Scanner Spectral 2-Photon scanning confocal microscope (Leica Microsystems), or Marianas Yokogawa type spinning disk confocal microscope with back-thinned EMCCD camera. Images were processed using Image J (US National Institutes of Health) and Adobe Photoshop software. Surface expression of endogenous GluA2 and GluN2B, and synaptic PSD95, was quantified using "sum of slice" *z* projections of images. Each field was background-subtracted and mean intensities calculated. Thresholded punctal size was analyzed using the Analyze Particle function in ImageJ.

Calculation of FRET efficiency. Images were acquired using Leica SP5 laser scanning confocal microscope operating with an argon laser tuned to 514nm, a DPSS laser tuned to 561nm, and a HeNe laser line tuned to 633nm. Cells were examined with a 63X 1.4 NA (Leica) oil immersion objective and 4X zoom. FRET was measured using the acceptor photobleaching method (5). Cells were bleached cells in the mCherry channel by scanning a region of interest 5-10 times using the 561nm DPSS laser line at 100% intensity. The time of bleach ranged from 3-10s depending on the size of the ROI for bleaching. For HEK293 cells, a scanning speed of 800Hz was used to maximize the degree of acceptor bleaching at each step. For neurons, a scanning speed of 8000Hz was used. Before and after each bleach step, Venus images were collected to assess changes in donor fluorescence. Because increases in Venus fluorescence caused by bleaching of the mCherry acceptor could potentially be masked by bleaching of Venus related simply to the imaging process itself, effect of photobleaching due to imaging was minimized by collecting Venus images at 1% of the laser intensity. To ensure that bleaching due to imaging was minimal, we monitored the level of bleaching in each experiment by collecting 5 images of the donor (Venus) prior to bleaching. The gain of the PMTs was adjusted so as to eliminate cross-talk and to achieve the best possible dynamic range.

To calculate the FRET energy transfer efficiency (E_T), we used the formula:

$$E_T = (1 - I_{da} / I_d) \qquad (1)$$

where I_{da} and I_d are the fluorescence intensities of the donor in the presence and absence of acceptor respectively. To obtain these values, fluorescence intensities were analyzed using Image J software and donor fluorescence variations were plotted against acceptor depletion over successive bleaching steps. The slope of the linear relationship was used to I_{da} and I_d. As

a reference, fluorescence of analogous peptides with only a donor, only an acceptor or both were measured to control for both pseudo FRET artifacts and intermolecular FRET. Average distance (r) between donor and acceptor was calculated using the formula:

$$r = R_0 (E_T^{-1} - 1)^{1/6} \qquad (2)$$

where R_0 is the Forster distance corresponding to 57Å for our Venus and mCherry sensors. This calculation assumes a random orientation factor ($\kappa^2 = 2/3$). To prepare HEK293 cells for FRET analysis, cells were fixed in 4% PFA/sucrose, washed in PBS, and mounted in 80% glycerol. To define regions of interest with cell markers (i.e. AMPARs, NMDARs, presynaptic markers, etc.), immunolabeling was performed with primary antibody, washed 3X, and labeled with an Alexa-647 or Alexa-750 conjugated secondary antibody, which was imaged on the Far Red or Far Far Red channel at the end of a photobleaching protocol. Images of these markers were used to create a mask to isolate regions for FRET analysis. 514-nm and 568-nm argon lasers were used to excite Venus and mCherry respectively (spectral channel settings: donor, 535nm ± 10nm; acceptor 610nm ± 25nm). Low resonant scanning at 800Hz was used in HEK293 cells experiments while high resonant scanning at 8000Hz was used for neuron experiments.

Immunoprecipitation and Immunoblot Analysis. Cells were pelleted by brief centrifugation, resuspended, washed once with PBS and solubilized in lysis buffer (150 mM NaCl, 5 mM EDTA pH 7.4, 50 mM Tris pH 7.4, 0.02% NaN_3) containing 1% Triton X-100 + NEM (2 mM), phenylmethanesulphonylfluoride (2 mM), leupeptin (10 g ml^{-1}), N-Tosyl-Lys-chloromethylketoneHCl (10 g ml^{-1}), chymotrypsin (10 g ml^{-1}) and pepstatin (10 g ml^{-1}). Following a 1 h solubilization (4 °C), samples were centrifuged at 14,000 *g* for 30 min at 4 °C. Subsequent analyses were performed using the Triton X-100–soluble fraction. Immunoprecipitations were performed by overnight antibody incubation at 4 °C. Protein-antibody complexes were isolated by incubation with Protein G–Sepharose for 3 h at 4 °C. For immunoblotting, proteins separated by SDS-PAGE were transferred to PVDF membranes. After transfer, the PVDF was blocked with 3% milk in wash buffer (10 mM Tris (pH 7.4), 0.05% Tween 20 (wt/vol) and 150 mM NaCl). Membranes were washed briefly in wash buffer and then incubated for 1 h with primary antibodies. The blots were washed and incubated with secondary antibody (goat antibody to mouse, rabbit or chicken Alexa-488, 568 or 647) at the appropriate dilution for 1 h. After washing, membranes were imaged on Bio-Rad Molecular Imager Pharos-FX (Biorad, Hercules, CA). Quantification was done using Image J (US National Institutes of Health).

PSD95 palmitoylation. The acyl-biotin exchange (ABE) method was performed as previously described (6). Click chemistry was performed with the alkyne-containing palmitate analog, 17-

ODYA, which was reacted with biotin-azide as previously described (7, 8). Cells were transfected with C3,5S-Ch-PSD95-V or Ch-PSD95-V alone, or with Ch-PSD95-V and Myc-DHHC2 (and palmostatin B treatment). At 24 hours following transfection, cells were deprived of fatty acids by incubating in media supplemented with charcoal-treated FBS (Sigma Aldrich) for 1 h prior to labeling. The 17-ODYA and palmitic acid were dissolved in DMSO to generate 100 mM stock solutions. To facilitate cellular uptake of fatty acids, prior to labeling, fatty acids were saponified by incubation with a 20% molar excess of potassium hydroxide at 65°C for 15 min. The saponified fatty acids were then dissolved in pre-warmed, serum-free culture media containing 20% fatty acid-free BSA at 37°C, followed by an additional 30 min incubation at 37°C. After deprivation of fatty acids, cells were washed with warm PBS and incubated in fresh media without supplement. BSA-conjugated fatty acids were added to cells in serum-free media (300ul fatty acid-BSA to 3ml of media). Cells were incubated with fatty acids for 5hr at 37°C to allow for metabolic labeling of proteins that are palmitoylated during the labeling period. Following labeling, cells were washed 3 times with PBS and then lysed in EDTA-free RIPA buffer. PSD95 was subsequently immunoprecipitated using anti-PSD95 antibody (Neuromab). Next, beads were reacted with biotin azide under standard click chemistry conditions, where EDTA-free RIPA buffer was mixed with 0.1 mM biotin azide, 0.1 mM TBTA, 1 mM TCEP, 1 mM $CuSO_4$. The click reaction mix was incubated with the beads in the dark at RT for 30min. Proteins were eluted and processed for SDS-PAGE and immunoblot analysis.

Statistical analysis. Results are expressed as mean ± SEM of *n* samples unless stated otherwise. Statistical significance was assessed by two-tailed Student's *t* test or ANOVA/Tukey *post hoc* as appropriate.

1. Claudio T (1992) Stable expression of heterologous multisubunit protein complexes established by calcium phosphate- or lipid-mediated cotransfection. *Methods Enzymol* 207:391-408.
2. Ho SN, Hunt HD, Horton RM, Pullen JK, & Pease LR (1989) Site-directed mutagenesis by overlap extension using the polymerase chain reaction. *Gene* 77(1):51-59.
3. Bresler T*, et al.* (2004) Postsynaptic density assembly is fundamentally different from presynaptic active zone assembly. *J Neurosci* 24(6):1507-1520.

4. Wu H, Reuver SM, Kuhlendahl S, Chung WJ, & Garner CC (1998) Subcellular targeting and cytoskeletal attachment of SAP97 to the epithelial lateral membrane. *J Cell Sci* 111 (Pt 16):2365-2376.
5. Kenworthy AK (2001) Imaging protein-protein interactions using fluorescence resonance energy transfer microscopy. *Methods* 24(3):289-296.
6. Drisdel RC & Green WN (2004) Labeling and quantifying sites of protein palmitoylation. *Biotechniques* 36(2):276-285.
7. Martin BR & Cravatt BF (2009) Large-scale profiling of protein palmitoylation in mammalian cells. *Nat Methods* 6(2):135-138.
8. Yap MC*, et al.* (2010) Rapid and selective detection of fatty acylated proteins using omega-alkynyl-fatty acids and click chemistry. *J Lipid Res* 51(6):1566-1580.

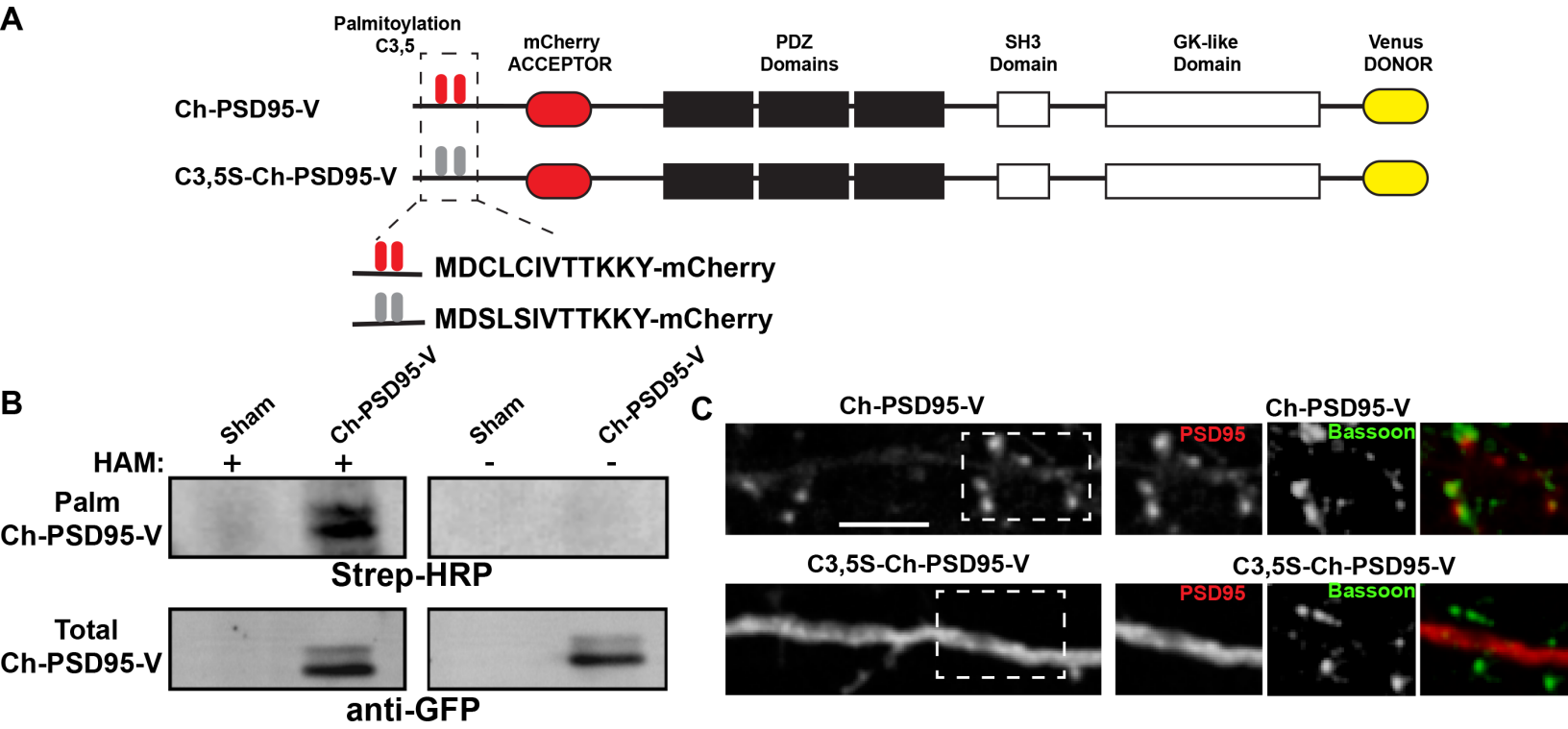
A
Palmitoylation
C3,5
mCherry
ACCEPTOR
PDZ
Domains
SH3
Domain
GK-like
Domain
Venus
DONOR
Ch-PSD95-V
C3,5S-Ch-PSD95-V
MDCLCIVTTKKY-mCherry
MDSLSIVTTKKY-mCherry
B
Sham
Ch-PSD95-V
Sham
Ch-PSD95-V
HAM:
+
+
-
-
Palm
Ch-PSD95-V
Strep-HRP
Total
Ch-PSD95-V
anti-GFP
C
Ch-PSD95-V
Ch-PSD95-V
PSD95
Bassoon
C3,5S-Ch-PSD95-V
C3,5S-Ch-PSD95-V
PSD95
Bassoon

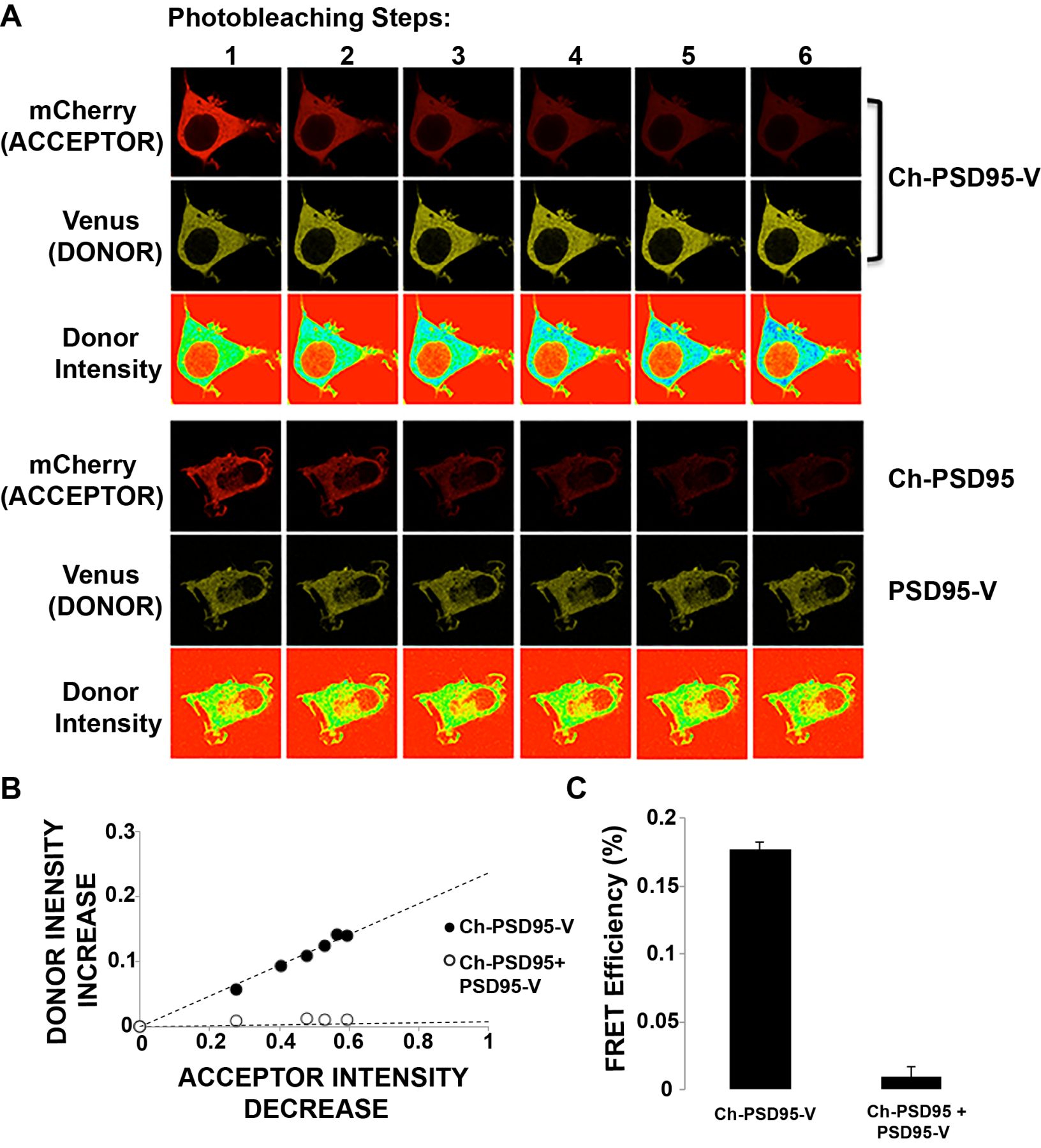
A
Photobleaching Steps:
1
2
3
4
5
6
mCherry (ACCEPTOR)
Venus (DONOR)
Donor Intensity
Ch-PSD95-V
mCherry (ACCEPTOR)
Venus (DONOR)
Donor Intensity
Ch-PSD95
PSD95-V
B
DONOR INENSITY INCREASE
0.3
0.2
0.1
0
0
0.2
0.4
0.6
0.8
1
ACCEPTOR INTENSITY DECREASE
Ch-PSD95-V
Ch-PSD95+ PSD95-V
C
FRET Efficiency (%)
0.2
0.15
0.1
0.05
0
Ch-PSD95-V
Ch-PSD95 + PSD95-V

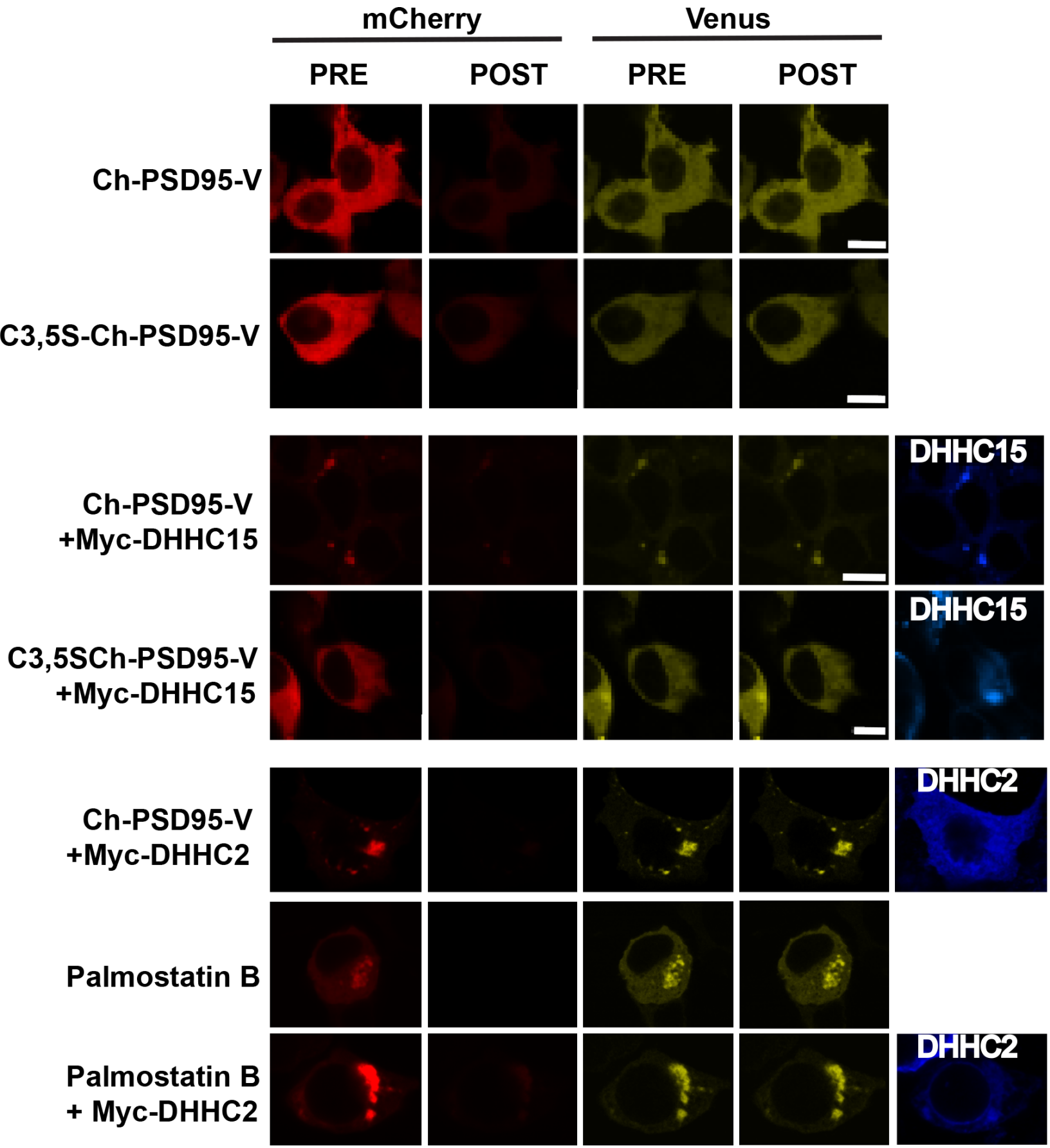
mCherry
Venus
PRE
POST
PRE
POST
Ch-PSD95-V
C3,5S-Ch-PSD95-V
Ch-PSD95-V
+Myc-DHHC15
DHHC15
C3,5SCh-PSD95-V
+Myc-DHHC15
DHHC15
Ch-PSD95-V
+Myc-DHHC2
DHHC2
Palmostatin B
Palmostatin B
+ Myc-DHHC2
DHHC2

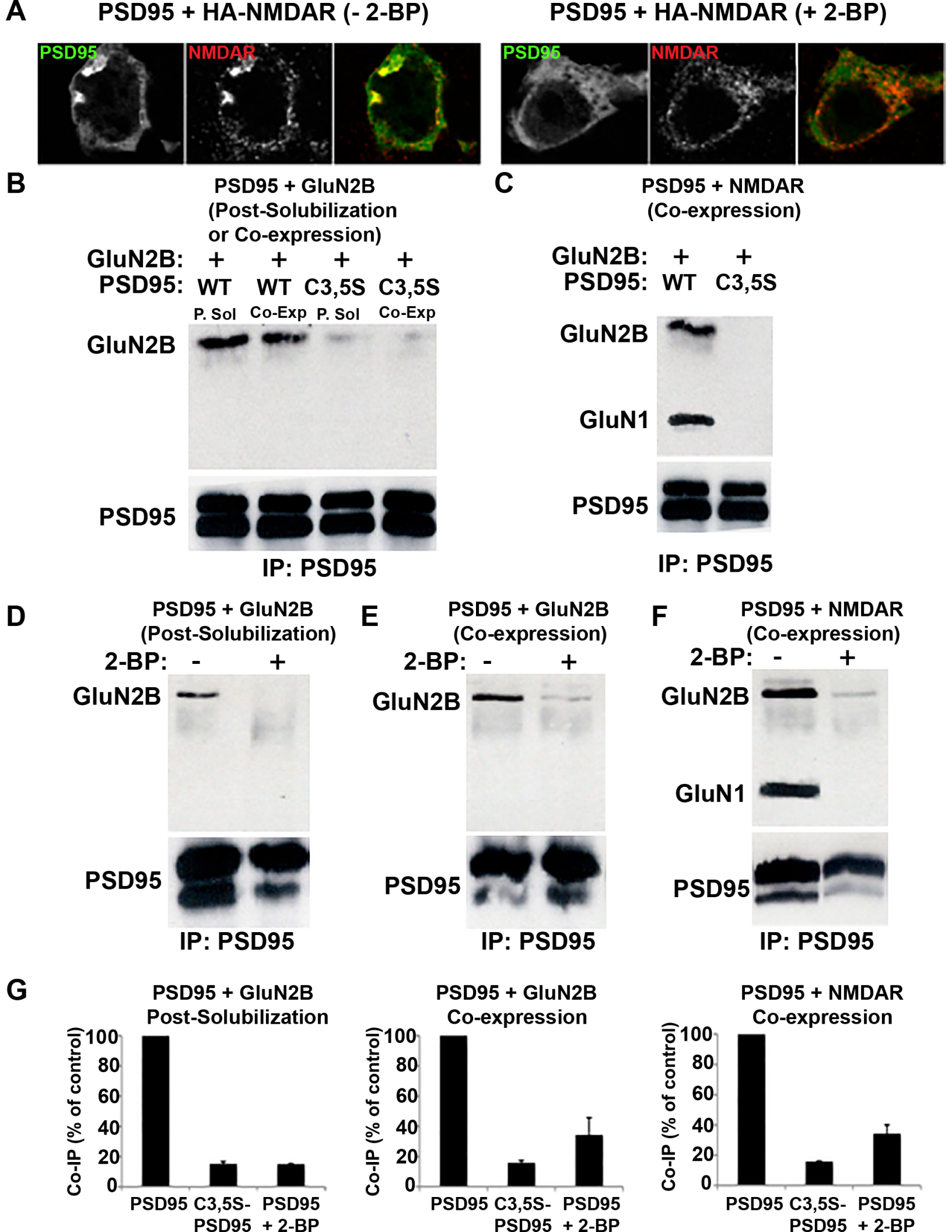
A
PSD95 + HA-NMDAR (- 2-BP)
PSD95 + HA-NMDAR (+ 2-BP)
PSD95
NMDAR
PSD95
NMDAR
B
PSD95 + GluN2B
(Post-Solubilization
or Co-expression)
GluN2B: + + + +
PSD95: WT WT C3,5S C3,5S
P. Sol Co-Exp P. Sol Co-Exp
GluN2B
PSD95
IP: PSD95
C
PSD95 + NMDAR
(Co-expression)
GluN2B: + +
PSD95: WT C3,5S
GluN2B
GluN1
PSD95
IP: PSD95
D
PSD95 + GluN2B
(Post-Solubilization)
2-BP: - +
GluN2B
PSD95
IP: PSD95
E
PSD95 + GluN2B
(Co-expression)
2-BP: - +
GluN2B
PSD95
IP: PSD95
F
PSD95 + NMDAR
(Co-expression)
2-BP: - +
GluN2B
GluN1
PSD95
IP: PSD95
G
PSD95 + GluN2B
Post-Solubilization
Co-IP (% of control)
100
80
60
40
20
0
PSD95
C3,5S-PSD95
PSD95 + 2-BP
PSD95 + GluN2B
Co-expression
Co-IP (% of control)
100
80
60
40
20
0
PSD95
C3,5S-PSD95
PSD95 + 2-BP
PSD95 + NMDAR
Co-expression
Co-IP (% of control)
100
80
60
40
20
0
PSD95
C3,5S-PSD95
PSD95 + 2-BP

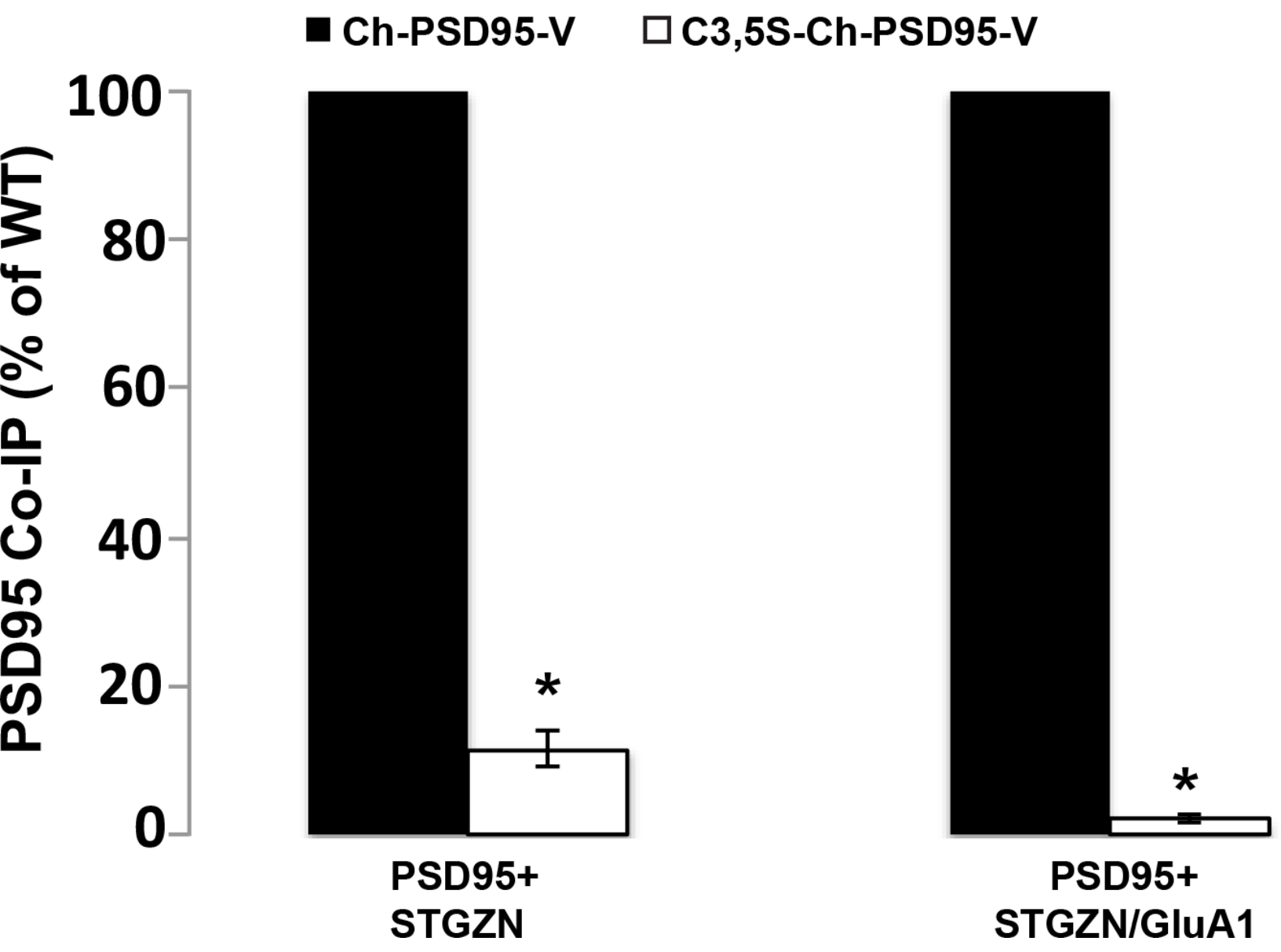
■ Ch-PSD95-V
□ C3,5S-Ch-PSD95-V
PSD95 Co-IP (% of WT)
100
80
60
40
20
0
*
*
PSD95+
STGZN
PSD95+
STGZN/GluA1